Title: Natural Radioactivity of Rocks from the Historic Jeroným Mine in the Czech Republic

Author: Dariusz Malczewski, Maria Dziurowicz, Zdenek Kalab, Marketa Rösnerová

UNIWERSYTET ŚLĄSKI
W KATOWICACH

Biblioteka
Uniwersytetu Śląskiego

Ministerstwo Nauki
i Szkolnictwa Wyższego

ORIGINAL ARTICLE

Natural radioactivity of rocks from the historic Jeroným Mine in the Czech Republic

Dariusz Malczewski[1] · **Maria Dziurowicz[1]** · **Zdenek Kalab[2,3]** · **Marketa Rösnerová[3]**

Abstract

This study reports the natural radioactivity of characteristic rocks found in the historic Jeroným Mine of the Czech Republic as measured under the laboratory conditions. The rocks analyzed included granites and schists weathered to varying degrees and collected from different levels of the underground workings of the Jeroným Mine. The mine itself has been subject to metal extraction (mainly tin and tungsten) since the sixteenth century and has recently been developed as a cultural and scientific attraction open to the public. Activity concentrations of ^{40}K, ^{232}Th and ^{238}U were measured from nine rock samples using gamma-ray spectrometry. The activity concentrations of ^{40}K varied from 595 Bq kg^{-1} to 1244 Bq kg^{-1}, while ^{232}Th varied from 25 Bq kg^{-1} to 55 Bq kg^{-1}. The activities associated with ^{238}U ranged from 46 Bq kg^{-1} to 386 Bq kg^{-1}. The measured activities were used to estimate two radiation hazard indices typically applied to building materials, the activity concentration index I and the external hazard index H_{ex}. Mean respective values of 1.02 and 0.77 for I and H_{ex} indicate that the rocks found in the Jeroným Mine meet radiological safety standards for building materials and do not pose a risk to potential tourists and staff.

Introduction

The historic Jeroným Mine is located near the former Čistá municipality (also known as Lauterbach Stadt) in the Sokolov District of the Czech Republic (Fig. 1). The locality is a part of a protected landscape, the Slavkovsky Les Mountains, which border the Bohemian Massif. The Bohemian Massif comprises part of the Variscan belt of Central Europe and hosts a number of uranium deposits found in both the Czech Republic and eastern Germany. Total historical uranium production reached approximately 350,000 t making the Bohemian Massif the most important uranium ore district in Europe (Kříbek et al. 2009). The Jeroným Mine represents a metalliferous deposit that yielded tin, tungsten, silver, gold, bismuth and uranium (Beran and Sejkora 2006). Mine workings date back to the first half of the sixteenth century and extraction occurred with interruptions until the early twentieth century. The nearby town of Čistá was impacted by several events after World War II and then later completely destroyed during a military training operation (Raška and Kirchner 2011). The long term subsurface mining activities and other human impacts have led to the designation of the Jeroným Mine as a National Heritage Site open to the public as part of the greater Czech Bavarian Jeopard.

Because World War II and post-war events destroyed archival documents and written records concerning the mine's history, large areas of the Jeroným Mine have not been evaluated for safety or access. The cessation of mining activities also led to flooding of some of the workings. The mining museum, opened in the twenty-first century, offers

✉ Dariusz Malczewski
dariusz.malczewski@us.edu.pl

Maria Dziurowicz
maria.dziurowicz@us.edu.pl

Zdenek Kalab
Zdenek.Kalab@ugn.cas.cz

Marketa Rösnerová
marketa.lednicka@ugn.cas.cz

1 Institute of Earth Sciences, University of Silesia, Będzińska 60, 41-200 Sosnowiec, Poland

2 Faculty of Civil Engineering, VSB - Technical University of Ostrava, Studentska 1768, 70800 Ostrava, Poruba, Czech Republic

3 Institute of Geonics, Czech Academy of Sciences, Studentska 1768, 70800 Ostrava, Poruba, Czech Republic

Fig. 1 The location of the Jeroným Mine on a map of the Czech Republic with recent photos of its access shafts and surroundings () *photos:* M. Rösnerová and Z. Kalab

access to mine workings and chambers which feature unique, historical tools and infrastructure (Žůrek and Kořínek 2001; Kaláb et al. 2006). Basic geological and geophysical analysis have been used to evaluate the safety of the site for visitors and museum workers. These studies have documented the structural condition and weathering of the rock massif in order to determine the stability of the mine (Lednická and Kaláb 2012, 2016). The mine itself extends to relatively shallow depths of only about 30–50 m below the surface. In preparation for opening of the site to the public, hydrological monitoring was also conducted to determine outflows, interconnections and the response of mine water levels to influent flows from intensive precipitation (Kaláb et al. 2010a, b). Hydrologic monitoring also addressed waters accumulated in closed, undrained areas of the mine.

The present study reports laboratory gamma-ray spectrometry measurements of natural radioactivity levels from characteristic rocks samples found in the mine. The ^{40}K, ^{232}Th and ^{238}U activity concentrations for representative granites and schists were compared to values obtained for similar rocks types as reported in the literature. Activity concentrations were also used to estimate standard indices

for assessing radiological safety of building materials and surroundings.

Geological setting and sample locations

Geologically, the Jeroným Mine accesses metamorphosed rocks belonging to the Slavkov mantle crystalline complex and Variscan granites of the Ore Mountains pluton. The area sampled occurred near the contact of major geological units, the Ore Mountain and Tepla-Barrandium megablock which formed at around 265 Ma. The immediate surroundings as well as the Jeroným Mine itself include altered acidic granites hosting prominent Variscan tin-tungsten mineralization. Intensive weathering and the age of the workings have destabilized some areas of the mine.

The Jeroným Mine is a shaft mine consisting of subsurface galleries, shafts and chambers spread across at least three horizontal levels ranging in depth from 10 to 50 m below the surface. Several recent papers have evaluated of structural stability of the mine (Froňka et al. 2013; Lednická and Kaláb 2013; Kaláb and Lednická 2016;

Lyubushin et al. 2014). The lowest level is permanently flooded making its scope is unknown. Some parts of the mine have been re-opened or recently developed. Intensive weathering and the age of the workings have destabilized other areas of the mine. Certain localities consist of fissured and weathered supporting pillars or roof layers in chambers. Figure 2 shows a sketch of the Jeroným Mine with sampling locations while Fig. 3 shows photos of typical sampling sites within the mine.

Fig. 2 Diagram of the Jeroným Mine with sampling locations marked. Table 1 lists sample descriptions
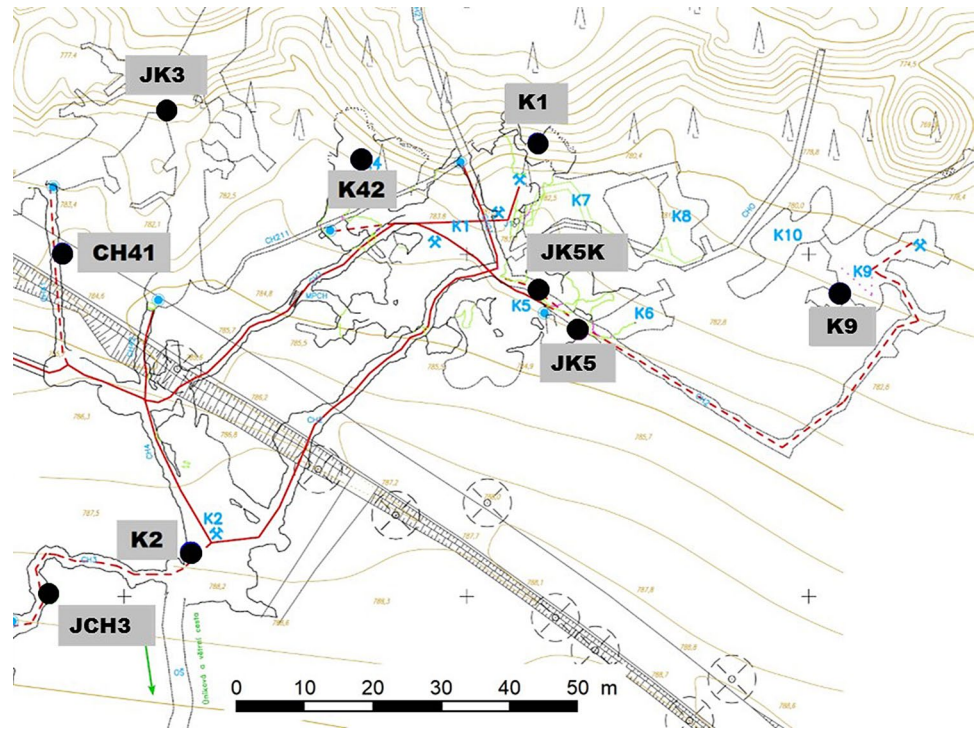
Fig. 3 Photos of typical sampling sites in the Jeroným Mine (*photos:* M. Rösnerová). **A** JK3 granite collection site from the pillar in a large chamber; **B** JK5 granite collection site from the seasonally flooded zone; **C** JK5K schist collection site from loose rock material; **D** JCH3 schist collection site from a gallery mined out during World War II.
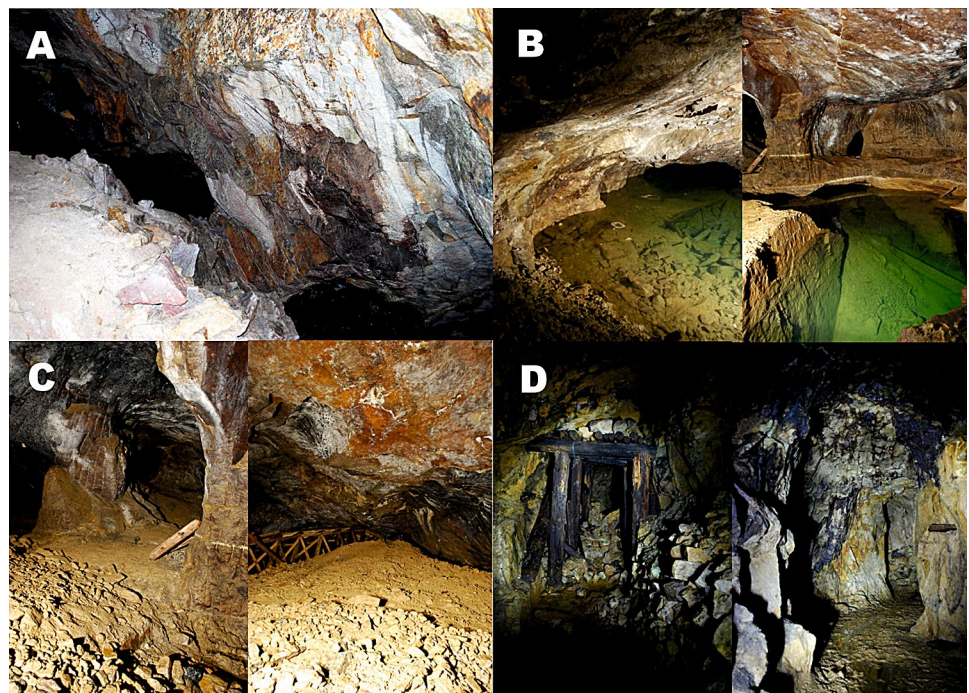
Materials and methods

Granite and schist samples from the Jeroným Mine were dried, crushed and placed in Marinelli-450 beakers. Samples were analyzed a few months after collection using a GX3020 HPGe detector in a lead and copper shield (60 mm) with a multichannel InSpector 2000 DSP buffer. The GX3020 HPGe system uses a coaxial HPGe Extended Range detector with 32% relative efficiency, a detector bias voltage of 3000 V and energy resolutions of 0.86 keV at 122 keV and 1.76 keV at 1332 keV. The LabSOCS (Laboratory Source-less Calibration Software) and Genie 2000 v.4 software packages performed efficiency calibration and estimated radionuclides and their activities. The spectrometer energy was calibrated using homogeneously dispersed ^{241}Am, ^{109}Cd, ^{139}Ce, ^{57}Co, ^{60}Co, ^{137}Cs, ^{113}Sn, ^{85}Sr, ^{88}Y and ^{203}Hg radioisotopes in a silicone resin [certificate source type Marinelli Beaker Standard Source (MBSS) supplied by the Czech Metrological Institute]. Activities for the target radionuclides were calculated from the following gamma transitions (energy in keV): ^{40}K (1460.8), ^{208}Tl (277.4, 583.1, 860.6 and 2614.5), ^{212}Pb (238.6 and 300.0), ^{214}Pb (241.9, 295.2 and 351.9), ^{214}Bi (609.3, 768.3, 1120.3 and 1764.5) and ^{228}Ac (338.3, 911.6, 964.6 and 969.1). A single measurement lasted 24 h. Measurements were performed at the Laboratory of Natural Radioactivity (Institute of Earth Sciences, University of Silesia). Figure 4 shows typical gamma-ray spectra for granite and schist samples JK3 and JCH3.

Results and discussion

Table 1 lists measured ^{40}K, ^{208}Tl, ^{212}Pb, ^{228}Ac, ^{214}Pb, ^{214}Bi, and ^{226}Ra activity concentrations for the nine Jeroným Mine rock samples.

^{40}K

As seen in Fig. 5 and Table 1, sample K9 (weathered granite) gave the lowest observed ^{40}K activity concentration of 595 Bq kg^{-1}. The granite K2 gave the maximum ^{40}K activity observed of 1244 Bq kg^{-1}. Weathered granite samples JK3 and K42 containing large, visible amounts of potassium feldspar gave the next highest ^{40}K values of 1141 Bq kg^{-1} and 1136 Bq kg^{-1} (respectively). Two schist samples JK5K and JCH3 gave similar ^{40}K activity concentrations of 1101 and 912 Bq kg^{-1}, respectively. Three other samples of weathered granite gave relatively low ^{40}K activity values ranging from 668 to 692 Bq kg^{-1}. These rock samples showed very little in the way of darker mineral content. As shown in Fig. 5, the average ^{40}K activity value of 907 Bq kg^{-1} slightly exceeds
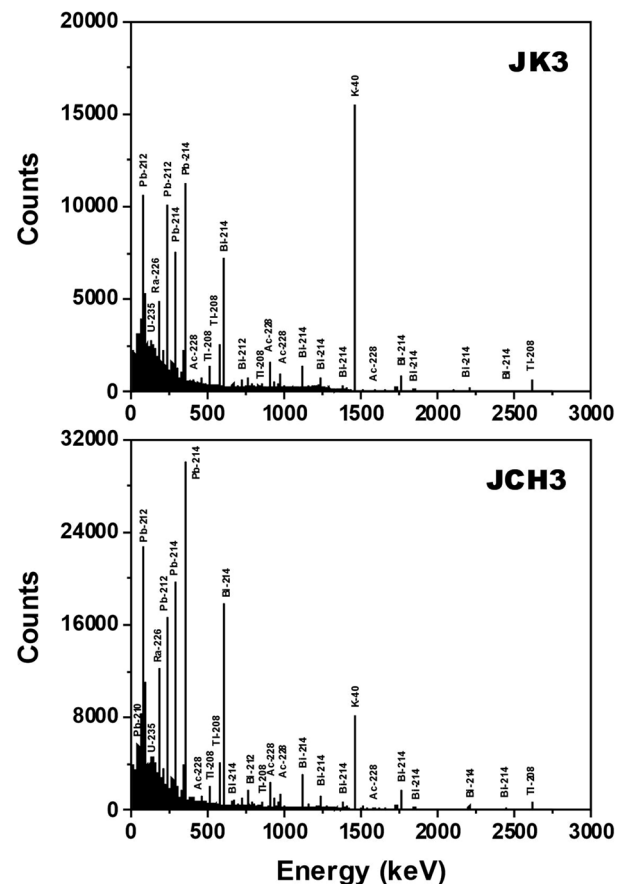
Fig. 4 Gamma-ray spectra from granite sample (JK3) and schist sample (JCH3). Characteristic gamma-ray emitters are marked above the corresponding peaks

the average ^{40}K activity concentration of 850 Bq kg^{-1} estimated for the continental crust (Eisenbud and Gessel 1997). This indicates that the study area is characterized by a normal ^{40}K radiation levels.

Granites

Figure 6 shows the ^{40}K activity concentrations for granite samples (excluding samples JK5K and JCH3), which gave an arithmetic mean value of 878 Bq kg^{-1}. As seen in Fig. 6, this value falls below the average value of 1200 Bq kg^{-1} reported for typical granites (Eisenbud and Gessel 1997; Van Schmus 1995) and below values of 1100 Bq kg^{-1} measured for Čistá type granites found in the study area (Krešl and Vaňková, 1978).

Albitized and greisenized granites K9, JK5 and K1 gave the lowest ^{40}K values observed from sampling sites located in the eastern part of the Jeroným Mine. The low values may reflect the albitization process in which the granites experienced hydration. A major increase in Na and loss of K could have resulted in considerably lower ^{40}K activity

Table 1 Activity concentrations of primordial radionuclides as measured in rock samples under laboratory conditions

Sample	Activity (Bq kg^{-1})						
	non-series	^{232}Th series			^{238}U series		
	^{40}K	^{208}Tl[a]	^{212}Pb	^{228}Ac	^{214}Pb	^{214}Bi	^{226}Ra[b]
K9 Weathered granite with a quartz vein	595 ± 25	7.4 ± 0.3	25.6 ± 1.5	25.2 ± 0.8	159 ± 7	147 ± 3	153 ± 8
JK5 Weathered granite from the seasonally flooded zone	668 ± 28	9.2 ± 0.3	30.1 ± 2.4	33.2 ± 0.9	408 ± 17	363 ± 6	386 ± 18
K1 Weathered granite	692 ± 29	8.2 ± 0.3	27.3 ± 2.2	26.9 ± 0.8	148 ± 6	131 ± 3	140 ± 7
JK5K schist from the seasonally flooded zone with infill materials	1101 ± 46	16.2 ± 0.4	53.6 ± 4.3	51.5 ± 1.2	203 ± 9	188 ± 4	196 ± 10
K42 Heavily weathered granite	1136 ± 92	10.5 ± 0.6	28.4 ± 3.2	26.6 ± 1.2	48 ± 4.1	44.7 ± 1.6	46.4 ± 4.4
K2 Granite	1244 ± 52	8.8 ± 0.3	30.1 ± 1.7	27.6 ± 0.8	150 ± 1	133 ± 2	142 ± 2
JK3 Weathered granite	1141 ± 47	8.2 ± 0.3	27.4 ± 2.2	28.3 ± 0.8	47.5 ± 2	43.9 ± 1.1	45.7 ± 2
CH41 Weathered granite	673 ± 28	8 ± 0.3	28.0 ± 1.6	27.4 ± 0.8	224 ± 10	206 ± 4	215 ± 11
JCH3 schist from the contact zone with granite	912 ± 38	17.1 ± 0.5	56.3 ± 4.5	55.1 ± 1.3	175 ± 7	159 ± 3	167 ± 8

[a]Branching ratio 36%

[b]Based on ^{214}Pb and ^{214}Bi activities
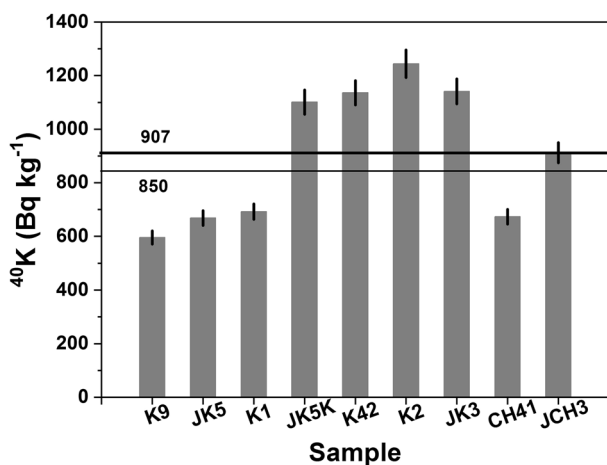
Fig. 5 Measured ^{40}K activity values. Thick solid line: average ^{40}K value measured from all samples. Thin solid line: average ^{40}K value reported for the continental crust
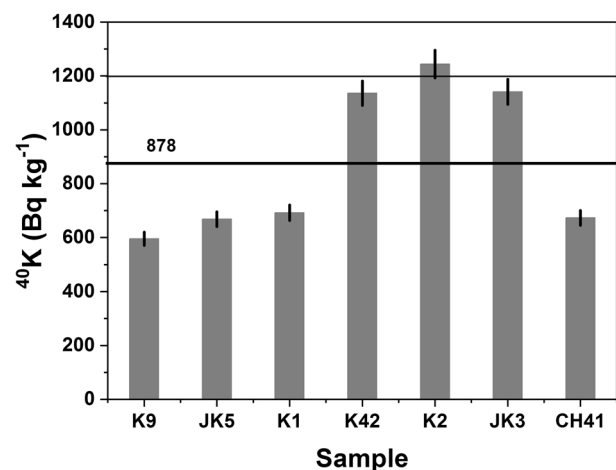
Fig. 6 Measured ^{40}K activities from granite samples (excluding schist samples JK5K and JCH3). Thick solid line: average ^{40}K activity measured from granite samples. Thin solid line: average ^{40}K activity reported for typical granites

values for these granite samples. The highest ^{40}K activity of 1244 Bq kg^{-1} (K2) slightly exceeded the average value for typical granites. This sample along with granites JK3 and K42 occurred in the western part of the mine.

Within measurement uncertainty, the average ^{40}K activity of 878 Bq kg^{-1} for granite samples strongly resembled the 887 Bq kg^{-1} average value determined from in situ measurements of Izera Block granites (Malczewski et al. 2004,

2005). Located 250 km away in SW Poland, the Izera Block exhibits similar geological structure to that of the Slavkovsky Les Mountains. The block also hosts metalliferous deposits of tin, cobalt, copper and bismuth. Laboratory measurements of a similar weathered granite from the Sławniowice quarry in the Opava Mountains (Poland) gave significantly higher ^{40}K activity values of 1560 Bq kg^{-1} (Dżaluk et al. 2018).

Papadopoulos et al. (2016) reported ^{40}K activity values ranging from 148 Bq kg^{-1} to 2518 Bq kg^{-1} with a mean value of 1097 Bq kg^{-1} for 70 samples of granites collected from plutons in western Anatolia (Turkey). Commercial granite rock used as building materials investigated by Pavlidou et al. (2006; 16 samples from Greece) and Tzortzis et al. (2003; 28 samples from Cyprus) gave mean ^{40}K activity values of 1104 Bq kg^{-1} and 1215 Bq kg^{-1}, respectively. Commercial granite samples from Brazil gave mean ^{40}K activity values ranging from 190 to 2029 Bq kg^{-1} and an arithmetic mean of 1320 Bq kg^{-1} (Anjos et al. 2011). One of the highest mean values reported for granite in the literature came from a rock in the Wadi Karim area of Egypt, which gave a ^{40}K activity value of 4849 Bq kg^{-1}. Samples collected in the Um Taghir region of Egypt (El-Arabi 2007) and from India, gave the maximum observed values of 10,230 and 10,990 Bq kg^{-1}, respectively.

Schists

The two schist samples, JK5K and JCH3, gave an average ^{40}K activity value of 1007 Bq kg^{-1}. This value slightly exceeds that measured from Izera Block schists (960 Bq kg^{-1}) using in situ methods (Malczewski et al. 2004 and 2005). It also exceeds values of 822 Bq kg^{-1} given for the USGS mica schist standard SDC-1.

### ^{232}Th series (^{228}Ac, ^{212}Pb, and ^{208}Tl)

Table 1 shows that rock samples have achieved radioactive equilibrium among ^{232}Th series daughter products. Since ^{228}Ac represents the second radionuclide in the thorium decay series, ^{232}Th activity is assumed to equal ^{228}Ac

activity. Figure 7 shows that sample K9 (weathered granite) gave the lowest ^{232}Th activity of 25 Bq kg^{-1}, whereas sample JCH3 (schist) gave the highest ^{232}Th activity value observed of 55 Bq kg^{-1}. All samples gave an average ^{232}Th activity value of 33 Bq kg^{-1}, which fell below the continental crust of 44 Bq kg^{-1}. This indicates relatively low and safe levels of background radiation within the Jeroným Mine.

Granites

The seven granite samples from the Jeroným Mine gave ^{232}Th activity values that fell within a narrow 25 Bq kg^{-1} (K9) to 33 Bq kg^{-1} (JK5) range. Figure 8 shows that the 28 Bq kg^{-1} arithmetic mean for these granites falls significantly below average ^{232}Th activity values or the 70 Bq kg^{-1} value reported for typical granites (Eisenbud and Gessel 1997). None of the ^{232}Th activities measured in this study exceeded this value. However, the average ^{232}Th activity exceeded mean values of 18 Bq kg^{-1} reported for Ĉistá type granites (Krešl and Vaňková, 1978). Similar to ^{40}K values, the average ^{232}Th activity for the Jeroným Mine granites resembled average values within uncertainties for Izera Block granites (29 Bq kg^{-1}) as measured by in situ methods (Malczewski et al. 2005). Granites from the easternmost part of the Sudetes (Opava Mountains) gave ^{232}Th values ranging from 7 (weathered granite) to 54 Bq kg^{-1} (granite) (Dżaluk et al. 2018). Papadopoulos et al. (2016) reported ^{232}Th activities ranging from 0.14 to 241 Bq kg^{-1} with a mean value of 90 Bq kg^{-1}. These values significantly exceeded average ^{232}Th values reported here for mine samples. Seven granite samples found in southeastern Eskisehir (Kaymaz, Turkey) gave higher values ranging from 165 to 352 Bq kg^{-1}
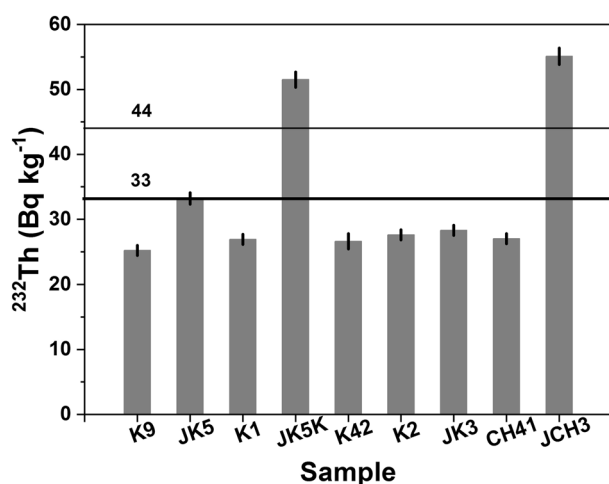
Fig. 7 Measured ^{232}Th activity values. Thick solid line: average ^{232}Th value from all samples. Thin solid line: average ^{232}Th value reported for the continental crust
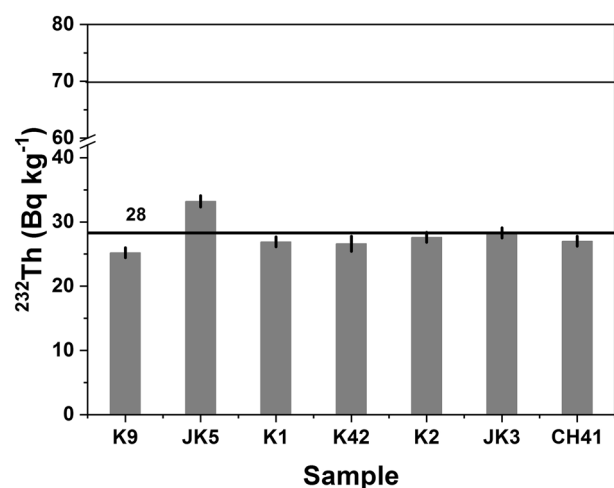
Fig. 8 Measured ^{232}Th activities from granite samples (excluding schist samples JK5K and JCH3). Thick solid line: average ^{232}Th activity from granite samples. Thin solid line: average ^{232}Th activity reported for typical granites

(average of 248 Bq kg^{-1}; Örgün et al. 2005). The highest ^{232}Th activity value reported (3834 Bq kg^{-1}) derived from anomalous granite samples from the Um Taghir region of Egypt (El-Arabi 2007).

The ^{232}Th activities measured from Jeroným Mine granites fell below activities measured from granites used as building materials and quarried from various global localities. Brazilian, Indian and Swedish commercial granites gave respective average ^{232}Th activity values of 106, 172 and 110 Bq kg^{-1} (Anjos et al. 2011; Chen and Lin 1996). Typical commercial granites from Greece and Sardinia gave respective ^{232}Th activity values of 77 and 66 Bq kg^{-1} (Papadopoulos et al. 2012; Dentoni et al. 2020). Commercial granites from Japan gave lower ^{232}Th activity values of 40 Bq kg^{-1} (Hassan et al. 2010).

Schists

Two schists (samples JK5K and JCH3) gave respective ^{232}Th activity values of 51 and 55 Bq kg^{-1} and an average value of 53 Bq kg^{-1}. These values exceed values measured from granites by as much as a factor of two. The values resemble those measured in situ from Izera Block schists (43 and 48 Bq kg^{-1}) (Malczewski et al. 2005). The 53 Bq kg^{-1} average for ^{232}Th activity values resembles the ^{232}Th activity reported for the USGS mica schist standard SDC-1 (46 Bq kg^{-1}).

^{238}U series (^{214}Pb, ^{214}Bi and ^{226}Ra)

Activity concentrations for ^{238}U were estimated assuming radioactive equilibrium within the $^{238}\text{U} \rightarrow ^{226}\text{Ra} \rightarrow ^{222}\text{R}$ n $\rightarrow ^{214}\text{Pb} \rightarrow ^{214}\text{Bi}$ decay chain. We estimated ^{238}U activities from ^{226}Ra activity determined from ^{214}Pb and ^{214}Bi activities.

Table 1 and Fig. 9 show that two weathered granites (JK3 and K42) gave the minimum ^{238}U activity value of 46 Bq kg^{-1}. The sample JK5 gave the maximum observed ^{238}U activity of 386 Bq kg^{-1}. All samples gave an average ^{238}U activity value of 166 Bq kg^{-1} which exceeds the continental crust of 36 Bq kg^{-1} (Eisenbud and Gessel 1997). The ^{238}U radiation background thus appears elevated relative to typical background.

Granite

Figure 10 shows granite sample ^{238}U activity concentrations that give an average value of 161 Bq kg^{-1}. This average exceeds average values for typical granites (40 Bq kg^{-1}) (Eisenbud and Gessel 1997) by a factor of four but falls slightly below the average value for Ĉistá type granites of 214 Bq kg^{-1} (Krešl and Vaňková, 1978). The nearby and geologically similar Izera Block hosts a leucogranite that
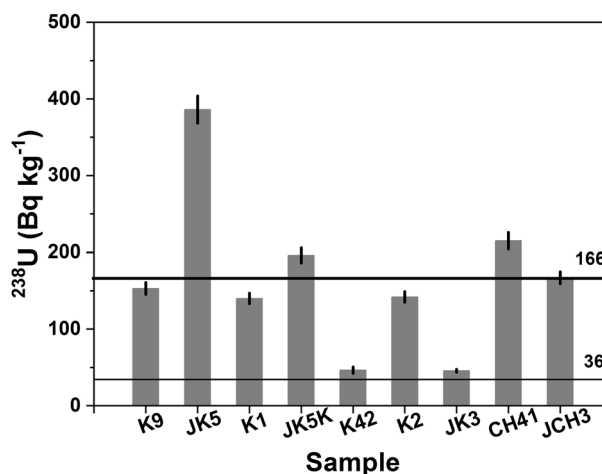
Fig. 9 Measured ^{238}U activity values. Thick solid line: average ^{238}U value from all samples. Thin solid line: average ^{238}U value reported for the continental crust
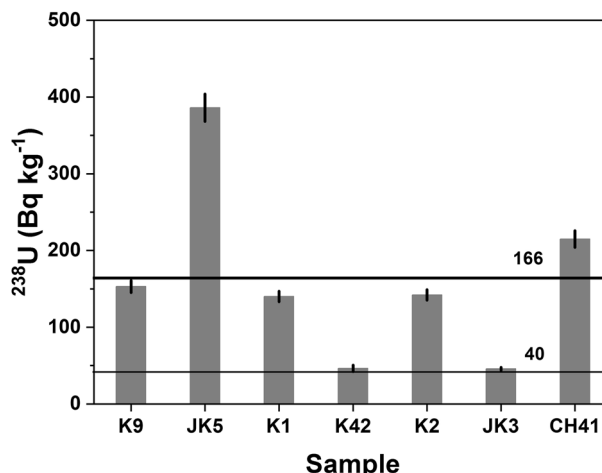
Fig. 10 Measured ^{238}U activities from granite samples (excluding schist samples JK5K and JCH3). Thick solid line: average ^{238}U activity from granite samples. Thin solid line: average ^{238}U activity reported for typical granites

gave the highest observed ^{238}U activity value of 120 Bq kg^{-1} (measured in situ) (Malczewski et al. 2005).

Samples JK3 and K42 gave the lowest observed ^{238}U activity value of 46 Bq kg^{-1}, which resembled that measured from typical granites. The sample JK5 gave the highest observed ^{238}U activity value of 386 Bq kg^{-1}. The difference between the highest and lowest values was 340 Bq kg^{-1}. Sample JK5 was a weathered granite collected from a chamber in the central part of the mine subject to seasonal flooding (Figs. 2 and 3). Four other granite samples exhibited relatively high ^{238}U activities of 215 Bq kg^{-1} for CH41, 153 Bq kg^{-1} for K9, 150 Bq kg^{-1} for K2 and 140 Bq kg^{-1}

for K1. Figures 2 and 10 show that the lowest ^{238}U activities observed come from samples collected from the northern part of the Jeroným Mine.

Table 2 lists ^{238}U activities for granites used as building materials from different global localities. Samples from Sardinia (Italy) gave the lowest mean value of 32.

Bq kg^{-1} (Dentoni et al. 2020). Granites from Egypt and India gave the highest mean values of 118 and 119 Bq kg^{-1} (Harb et al. 2012; Chen and Lin 1996). Tzortzis et al. (2003) reported an average value of 77 Bq kg^{-1} and ^{238}U concentrations of up to 588 Bq kg^{-1} for rocks from Cyprus. Sakoda et al. (2008) analyzed granite samples from Misasa (Japan) and Badgastein (Austria), which both host well-known radon therapy spas. Those samples gave extremely high ^{226}Ra (^{238}U) activity concentrations of 895 Bq kg^{-1} for the Misasa granite and 7064 Bq kg^{-1} for the Badgastein granite. For comparison, the JK5 granite from the Jeroným Mine gave a ^{238}U activity concentration of 386 Bq kg^{-1}. Granites from the Um Taghir region (eastern desert, Egypt) gave the highest ^{238}U activity

concentration value reported in the literature of 9087 Bq kg^{-1} (El-Arabi 2007).

Schists

Schist samples from the Jeroným Mine gave ^{238}U activities of 167 Bq and 196 Bq kg^{-1} with an average value of 181 Bq kg^{-1}, which slightly exceeds that measured from the granite samples. This value also greatly exceeded the 36 Bq kg^{-1} value measured from the Clarke (Eisenbud and Gessel 1997) (Fig. 9), the 38 Bq kg^{-1} value measured from USGS standard SDC-1 and the 43 Bq kg^{-1} value measured in situ for Izera Block schists (Malczewski et al. 2004, 2005).

Radiological hazard assessment

Basic indices used to evaluate building materials provided estimates and dose criteria for the radiological hazards related to mine tours and working conditions. The European Union standard index *I*, as defined in Council Directive 59 (2013), represents the sum of three isotopic fractions expressed as:

$$I = \frac{A_{Ra}}{300 Bqkg^{-1}} + \frac{A_{Th}}{200 Bqkg^{-1}} + \frac{A_K}{3000 Bqkg^{-1}}$$

where A_{Ra}, A_{Th} and A_K represent ^{226}Ra, ^{232}Th and ^{40}K (Bq kg^{-1}) activities in surroundings or building material (EC RP 112 1999; Nuccetelli et al. 2012). Bulk material amounts give indoor dose rate which should not exceed a value of 1 mSv y^{-1} (unity). Table 3 and Fig. 11 show calculated *I* values along with individual ^{226}Ra, ^{232}Th and ^{40}K contributions for rock samples analyzed in this study.

The external hazard index H_{ex} also represents a commonly used index for evaluating radiological risk of building materials. It is calculated as follows:

$$H_{ex} = \frac{A_{Ra}}{370 Bqkg^{-1}} + \frac{A_{Th}}{259 Bqkg^{-1}} + \frac{A_K}{4810 Bqkg^{-1}}$$

where A_{Ra}, A_{Th} and A_K represent ^{226}Ra, ^{232}Th and ^{40}K (Bq kg^{-1}) activities in the building material or surroundings

Table 2 Examples of ^{226}Ra (^{238}U) activities measured from commercial granites used in construction from different global localities

| Reference	Locality	^{226}Ra (^{238}U)
Chen and Lin 1996	India	119[a]
		68–160[b]
Chen and Lin 1996	Sweden	107
		102–111
Tzortzis et al. 2003	Cyprus	77
		1–588
Anjos et al. 2011	Brazil	45
		5–160
Harb et al. 2012	Egypt	118
		55–212
Papadopoulos et al. 2012	Greece	84
		27–229
Dentoni et al. 2020	Sardinia, Italy	36
		18–80

[a] Average

[b] Range

Table 3 Calculated *I* and H_{ex} index values with contributions from ^{40}K, ^{232}Th and ^{226}Ra components as measured from Jeroným Mine samples

Sample	I_K	I_{Th}	I_{Ra}	I	H_K	H_{Th}	H_{Ra}	H_{ex}
K9	0.20	0.13	0.51	0.83	0.12	0.10	0.41	0.63
JK5	0.22	0.17	1.29	1.68	0.14	0.13	1.04	1.31
K1	0.23	0.13	0.47	0.83	0.14	0.10	0.38	0.63
JK5K	0.37	0.26	0.65	1.28	0.23	0.20	0.53	0.96
K42	0.38	0.13	0.15	0.67	0.24	0.10	0.13	0.46
K2	0.41	0.14	0.47	1.03	0.26	0.11	0.38	0.75
JK3	0.38	0.14	0.15	0.67	0.24	0.11	0.12	0.47
CH41	0.22	0.14	0.72	1.08	0.14	0.10	0.58	0.83
JCH3	0.30	0.28	0.56	1.14	0.19	0.21	0.45	0.85
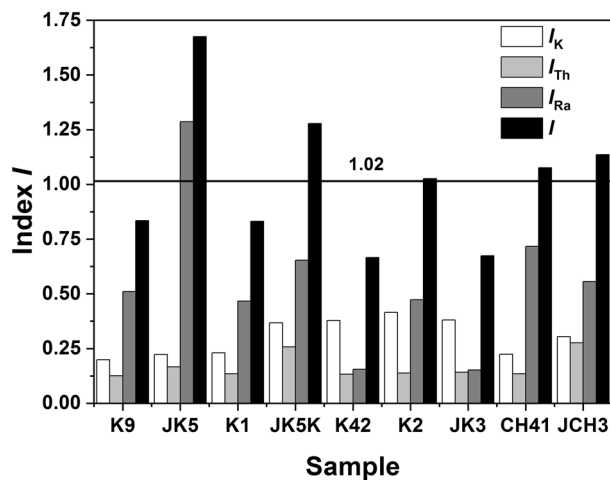
Fig. 11 Calculated I index values showing contributions from ^{40}K (I_K), ^{232}Th (I_{Th}) and ^{226}Ra (I_{Ra}) components. The solid line shows the average value for all samples
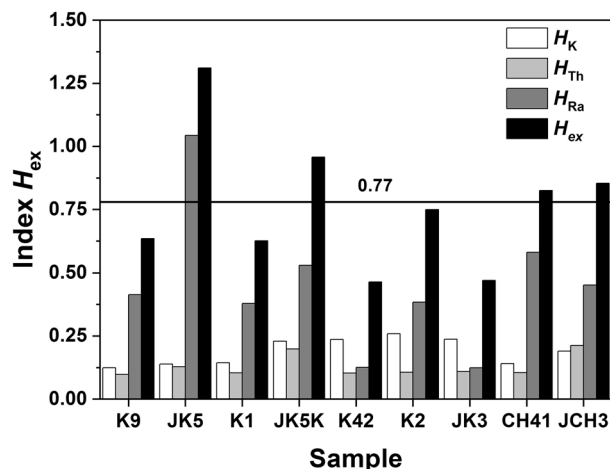
Fig. 12 Calculated H_{ex} index values showing contributions from ^{40}K (H_K), ^{232}Th (H_{Th}) and ^{226}Ra (H_{Ra}) components. The solid line shows the average value for all samples

as before. An H_{ex} index equal to unity corresponds to an external gamma dose of 1.5 mSv y^{-1} from a material. The H_{ex} utilizes principles of radium equivalent activity (Ra_{eq}). The estimate assumes equivalent gamma-ray dose rate produced by 370 Bq kg^{-1} for ^{226}Ra, 259 Bq kg^{-1} for ^{232}Th and 4810 Bq kg^{-1} for ^{40}K (Beretka and Mathew 1985; Monged et al. 2020). Table 3 and Fig. 12 list H_{ex} estimates for the rock samples analyzed here.

As seen in Table 3 and Fig. 11, only the JK5 granite sample exceeded critical values of 1 for index I ($I = 1.68$). Samples JK5K, JCH3, CH41 and K2 slightly exceeded the critical value and all samples gave an average I of 1.02. This average I value fell to 0.94 when JK5 was excluded from

calculation. The critical $I = 1$ threshold corresponding to the dose of 1 mSv derives from an annual exposure time of 7000 h. For the seven samples analyzed, ^{226}Ra made the largest contribution to the I estimate. For the two remaining samples of K42 and JK3, ^{40}K made the largest contribution to I. For all samples, ^{232}Th made the lowest contribution to I.

Similar to the I index, the H_{ex} index exceeded unity only for the JK5 granite sample, which gave a $H_{ex} = 1.3$ (Tab. 3, Fig. 12). The remaining samples gave H_{ex} values of less than one. All samples gave an average H_{ex} value of 0.77. The largest contribution to H_{ex} values again came from ^{226}Ra except for the two samples K42 and JK3, for which the largest contribution came from ^{40}K. The calculated H_{ex} values for the Jeroným Mine rocks resemble typical values calculated for granites used in construction. For example, commercial granites from Italy, Greece and Sweden give average H_{ex} values of 0.56, 0.73 and 0.97, respectively. Granites from Japan give H_{ex} values ranging from 0.33 to 1.88 with an average value of 0.66 (Hassan et al. 2010). Granites from Egypt gave H_{ex} values ranging from 0.7 to 1.77 with an average value of 1.12 (Harb et al. 2012).

Conclusions

Granites and schists from the Jeroným Mine gave mean activity values for ^{40}K, ^{232}Th and ^{238}U of 907, 33 and 166 Bq kg^{-1}, respectively. Average ^{226}Ra (^{238}U) activity concentrations exceeded average values measured for typical granites and schists. The estimates of I and H_{ex} indices used to assess radiological hazard indicate that the rocks from Jeroným Mine represent safe environmental materials. Gamma ray radiation from the rock surroundings in the Jeroným Mine does not pose a risk to potential tourists and staff. Future analyses should include in situ radon measurements to confirm the low level of the radiological risk.

References

Anjos RM, Juri Ayub J, Cid AS, Cardoso R, Lacerda T (2011) External gamma-ray dose rate and radon concentration in indoor environments covered with Brazilian granites. J Environ Radioact 102:1055–1061. https://doi.org/10.1016/j.jenvrad.2011.06.001

Beran P, Sejkora J (2006) The Krásno Sn-W ore district near Horni Slavkov: mining history, geological and mineralogical characteristics. J Czech Geol Soc 51(1–2):3–42

Beretka J, Mathew PJ (1985) Natural radioactivity of Australian building materials, industrial wastes and by-products. Health Phys 48(1):87–95

Chen CJ, Lin YM (1996) Assessment of building materials for compliance with regulations of ROC. Environ Int 22:221–226

Council Directive (2013) EU 2013/59/Euratom. Laying down basic safety standards for protection against the dangers arising from exposure to ionising radiation

Dentoni V, Da Pelo S, Aghdam MM, Randaccio P, Loi A, Careddu N, Bernardini A (2020) Natural radioactivity and radon exhalation rate of Sardinian dimension stones. Constr Build Mater 247:18377. https://doi.org/10.1016/j.constrbuildmat.2020.118377

Dżaluk A, Malczewski D, Żaba J, Dziurowicz M (2018) Natural radioactivity in granites and gneisses of the Opava Mountains (Poland): a comparison between laboratory and in situ measurement. J Radioanal Nucl Chem 316(1):101–109. https://doi.org/10.1007/s10967-018-5726-3

Eisenbud M, Gessel T (1997) Environmental radioactivity from natural, industrial and military sources. Academic Press, San Diego

El-Arabi AM (2007) 226Ra, 232Th and 40K concentrations in igneous rocks from Eastern Desert Egypt and its radiological implications. Radiat Meas 42:94–100. https://doi.org/10.1016/j.radmeas.2006.06.008

European Commission (1999) Radiation Protection 112 Radiological Protection Principles Concerning the Natural Radioactivity of Building Materials (Luxembourg: European Union) http://ec.europa.eu/energy/nuclear/radiationprotection/doc/publication/112.pdf

Froňka A, Hradecký J, Kaláb Z, Lednická M (2013) Initial recording of the radon activity concentration in Jeroným mine. Int J Explor Geophys Remote Sens Environ 1:44–52

Harb S, Abbady A, El-Kamel AH, Saleh II, El-Mageed AI (2012) Natural radioactivity and their radiological effects for different types of rocks from Egypt. Radiat Phys Chem 81(3):221–225. https://doi.org/10.1016/j.radiatphyschem.2011.11.005

Hassan NM, Ishikawa T, Hosoda M, Sorimachi A, Tokonami S, Fukushi M, Sahoo SK (2010) Assessment of the natural radioactivity using two techniques for the measurement of radionuclide concentration in building materials used in Japan. J Radioanal Nucl Chem 283:15–21. https://doi.org/10.1007/s10967-009-0050-6

Kaláb Z, Lednická M (2016) Long-term Geomechanical observation in the Jeroným Mine. Acta Geophys 64(5):513–1524. https://doi.org/10.1515/acgeo-2016-0054

Kaláb Z, Knejzlík J, Kořínek R, Žůrek, P (2006) Cultural monument Jeroným Mine, Czech Republic – Contribution to the Geomechanical Stability Assessment, Publs Inst Geophys Pol Acad Sc M-29(395):137–146

Kaláb Z, Lednická M, Hrubešová E (2010a) Seismic activity in medieval Jeroným Mine, west Bohemia, during period 2006–2009. Górnictwo i Geologia 5(2):67–77

Kaláb Z, Lednická M, Knejzlik J, Telesca L (2010b) First results from long-term monitoring of distance using a laser distance meter in shallow medieval mine. Acta Geodyn Geomater 7(4):469–473

Krešl M, Vaňková V (1978) Radioactivity and heat production data from several boreholes in the Bohemian Massif. Studia Geophys Geod 22:165–176. https://doi.org/10.1007/BF01614041

Kříbek B, Žák K, Dobeš P, Leichmann J, Pudilová M, René M, Scharm B, Scharmová M, Hájek A, Holeczy D, Hein UF, Lehmann B (2009) The Rožná uranium deposit (Bohemian Massif, Czech Republic): shear zone-hosted, late Variscan and post-Variscan hydrothermal mineralization. Miner Deposita 44:99–128. https://doi.org/10.1007/s00126-008-0188-0

Lednická M, Kaláb Z (2012) Evaluation of granite weathering in the Jeroným Mine using non-destructive methods. Acta Geodyn Et Geomater 9(2):211–220

Lednická M, Kaláb Z (2013) Vibration effect of earthquakes in abandoned medieval mine. Acta Geod Geophys 48(3):221–234. https://doi.org/10.1007/s40328-013-0018-4

Lednická M, Kaláb Z (2016) Determination of granite rock massif weathering and cracking of surface layers in the oldest parts of medieval mine depending on used mining method. Arch Min Sci 61(2):381–395. https://doi.org/10.1515/amsc-2016-0028

Lyubushin AA, Kaláb Z, Lednická M (2014) Statistical properties of seismic noise measured in underground spaces during seismic swarm. Acta Geod Geophys 49(2):209–224. https://doi.org/10.1007/s40328-014-0051-y

Malczewski D, Teper L, Dorda J (2004) Assessment of natural and anthropogenic radioactivity levels in rocks and soils in the environs of Swieradow Zdroj in Sudetes, Poland, by in situ gamma-ray spectrometry. J Environ Radioact 73:233–245. https://doi.org/10.1016/j.jenvironradioact.2003.08.010

Malczewski D, Sitarek A, Żaba J, Dorda J (2005) Natural radioactivity of selected crystalline rocks of the Izera Block (Sudetes, SW Poland). [in Polish: Promieniotwórczość naturalna wybranych skał krystalicznych bloku izerskiego]. Przegląd Geologiczny 53(3):237–244

Monged MHE, Abu Khatita AM, El-Hemamy ST, Sabet HS, Al-Azhary MAE (2020) Environmental assessment of radioactivity levels and radiation hazards in soil at North Western-Mediterranean Sea coast. Egypt Environ Earth Sci 79:386. https://doi.org/10.1007/s12665-020-09131-y

Nuccetelli C, Risica S, D'Alessandro M, Trevisi R (2012) Natural radioactivity in building material in the European Union: robustness of the activity concentration index I and comparison with a room model. J Radiol Prot 32:349–358. https://doi.org/10.1088/0952-4746/32/3/349

Örgün Y, Altinsoy N, Gültekin AH, Karahan G, Çelebi N (2005) Natural radioactivity levels in granitic plutons and groundwaters in Southeast part of Eskisehir, Turkey. Appl Radiat Isot 63:267–275. https://doi.org/10.1016/j.apradiso.2005.03.008

Papadopoulos A, Christofides G, Koroneos A, Stoulos S, Papastefanou C (2012) Natural radioactivity and dose assessment of granitic rocks from the Atticocycladic Zone (Greece). Periodico Di Mineralogia 81(3):301–311. https://doi.org/10.2451/2012PM0017

Papadopoulos A, Altunkaynak Ş, Koroneos A, Ünal A, Kamaci Ö (2016) Distribution of natural radioactivity and assessment of radioactive dose of Western Anatolian plutons, Turkey. Turkish J Earth Sci 25:434–455. https://doi.org/10.3906/yer-1605-5

Pavlidou S, Koroneos A, Papastefanou C, Cristofides G, Stoulos S, Vavelides M (2006) Natural radioactivity of granites used as building materials. J Environ Radioact 89:48–60. https://doi.org/10.1016/j.jenvrad.2006.03.005

Raška P, Kirchner K (2011) Assessing landscape changes in a region affected by military activity and uranium mining (Prameny Municipality Area, Western Bohemia, Czech Republic): a multi-scale approach. Morav Geogr Rep 19(4):28–37

Sakoda A, Hanamoto K, Ishimori Y, Nagamatsu T, Yamaoka K (2008) Radioactivity and radon emanation fraction of the granites samples at Misasa and Badgastein. Appl Radiat Isot 66:648–652. https://doi.org/10.1016/j.apradiso.2007.11.015

Tzortzis M, Tsertos H, Christofides S, Christodoulides G (2003) Gamma measurements and dose rates in commercially used tiling rocks

(granites). J Environ Radioact 70(3):223–235. https://doi.org/10.1016/SO265-931X(03)00106-1

Van Schmus WR (1995) Natural radioactivity of the crust and mantle. In: Ahrens TJ (Ed.), Global Earth Physics. American Geographical Union, Washington DC, 282–291, https://doi.org/10.1029/RF001p283.

Žůrek P, Kořínek R (2001) Opening of the Medieval Jeroným Mine in the Czech Republic to the Public. Journal of Mining & Geological Science 40–41:51–72